Temporal variation in groundwater hydrochemistry driven by natural and anthropogenic processes at a reclaimed water irrigation region

Yajun Wang, Xianfang Song, Binghua Li, Ying Ma, Yinghua Zhang, Lihu Yang, Hongmei Bu and Peter E. Holm

ABSTRACT

Long-standing wastewater and reclaimed water irrigation systems degrade groundwater quality and thus pose great risks to local soils and even to human health. In this study, seasonal variations in hydrochemical characteristics of groundwater were assessed to determine possible processes that induce groundwater degradation. Beijing was used as the focus area. A total of 82 wells at the southeast irrigation region of Beijing were investigated in 2014. Descriptive statistics, correlation analysis, Piper diagram, and saturation indices were used to distinguish seasonal variations in hydrochemistry in shallow and deep groundwater and possible reclaimed water irrigation effects. The main natural controlling processes include mineral precipitation and dissolution, cation exchange reactions, and dilution effects in shallow and deep groundwater. However, cation exchange reactions are considered to be intense in deeper aquifer. Additionally, shallow groundwater sites subjected to salinization and nitrate contamination were associated with intensive agricultural input and reclaimed water leaching. Sites continuously contaminated by nitrate were mainly distributed on highly permeable sediments. Irrigation with deep groundwater may reduce soil drainage conditions due to a high percentage of sodium. Overall, seasonal replenishment for subterranean quaternary aquifers from rainfall or irrigation plays a vital role in seasonal variation in shallow groundwater hydrochemistry.

Key words | Beijing, groundwater hydrochemistry, reclaimed water irrigation region, seasonal variation

Yajun Wang
Xianfang Song (corresponding author)
Ying Ma
Yinghua Zhang
Lihu Yang
Hongmei Bu
Key Laboratory of Water Cycle and Related Land Surface Processes, Institute of Geographic Sciences and Natural Resources Research, Chinese Academy of Sciences,
11A, Datun Road, Chaoyang District, Beijing 100101, China
E-mail: *songxf@igsnrr.ac.cn*

Yajun Wang
Sino-Danish Center for Education and Research, Chinese Academy of Sciences,
Beijing 100190, China

Yajun Wang
Xianfang Song
College of Resources and Environment, University of Chinese Academy of Sciences,
19A Yuquan Road, Beijing 100049, China

Binghua Li
Beijing Water Science and Technology Institute,
21 Chegongzhuangxi Road, Haidian District, Beijing 100000, China

Peter E. Holm
Section for Environmental Chemistry and Physics, University of Copenhagen,
Thorvaldsensvej 40, Frederiksberg C, Copenhagen 1871, Denmark

INTRODUCTION

Growing human population, urbanization, expanding agricultural production, and climate change have created large water demands beyond local region supply capacity, especially in undeveloped and developing nations (Vorosmarty *et al.* 2010). The North China Plain experiences groundwater resource depletion because 70–80% of its irrigation systems rely on groundwater (Cao *et al.* 2016). For the alleviation of groundwater scarcity, supply-led engineering solutions, such as reclaimed water utilization, were established. Reclaimed water is integrated into the local planning and development of water resource as a substitute for groundwater as a result of the economic and environmental benefits (Chen *et al.* 2013). However, groundwater quality deterioration caused by long-term irrigation using wastewater and reclaimed water has aroused considerable concern. Emerging contaminants, priority substances,

doi: 10.2166/nh.2018.123

pathogenic microorganisms, eutrophication, and heavy metals in groundwater are extensively reported and mainly correspond to the effluents of wastewater treatment plants (WTPs) (Katz *et al.* 2009; Xu *et al.* 2010; Jurado *et al.* 2012). In northern China, cities such as Beijing, Tianjin, and Shijiazhuang that use reclaimed water for agriculture and landscaping have made efforts to investigate contaminants in reclaimed water, soil and receiving groundwater. Contaminants have low concentration levels in groundwater and thus their posed risks are considerably less compared with those posed by surface water and soils. The low concentration levels of contaminants are possibly related to an unsaturated zone chemical buffer effect and aquifer natural attenuation capacity (Candela *et al.* 2007). However, salinization, nitrate contamination and hydrochemistry variation in groundwater underneath wastewater and reclaimed water irrigation region remain as widespread environmental hazards in many regions.

The concentrations of some ions (nitrate, sodium, nitrite, boron and chloride) in groundwater downstream of WTPs in northern Florida, USA, are higher than at upstream and decrease with distance from the WTPs (Katz *et al.* 2009). In the Mediterranean Coastal Aquifer, salinity pollution is affected by conjoined factors such as seawater interaction, lithology, and reclaimed water irrigation (Kass *et al.* 2005; Anane *et al.* 2014). Nitrate concentrations in groundwater from land receiving reclaimed water are elevated because of denitrification in the vadose zone caused by ammonium in wastewater, this increase results in groundwater acidification (Kass *et al.* 2005). A study from north eastern Tunisia reported that cropping density and conjunction factors, rather than reclaimed water, are the influential factors in nitrate and salinity contamination in groundwater (Anane *et al.* 2014).

Groundwater chemistry is largely determined by natural hydrogeochemical and hydrophysical processes and anthropogenic interferences. However, hydrochemical characteristics of groundwater under seasonal alteration in reclaimed water irrigation areas are rarely explored. Groundwater chemistry changes only slightly between seasons in arid regions, but obvious variations were observed in coastal regions due to human-effected recharge during no-crop growing season (Carroll *et al.* 2013; Re *et al.* 2014), evapotranspiration and precipitation events (Isa *et al.* 2014; Yan *et al.* 2015). In northern China, few studies were conducted on seasonal evolution of groundwater quality under reclaimed water irrigation and associated dominating factors.

Based on the determined physicochemical data, the hydrochemical methods of integrated statistical analysis application, Piper diagram, correlation analysis, ionic ratios and saturation index are widely used for elucidating groundwater quality evolution and identifying variation-driving factors. Other methods applied for mechanism studies are the isotopic trace method (Chen *et al.* 2006; Surinaidu 2016), ensemble learning model (Singh *et al.* 2014), and numerical simulation (Foppen 2002; Han *et al.* 2015).

In the present study, we focused on the Quaternary alluvium aquifers in southeastern Beijing, North China. In this area, irrigation using wastewater has been utilized for 40 years and reclaimed water has been used for 10 years. These processes caused potential environmental concerns with respect to the local groundwater. In the present study, chemical and physical parameters from 164 groundwater samples at different aquifers in both dry and wet season were investigated using multiple statistical methods and graphical plots analyses. The study has the following main objectives: (1) to investigate groundwater hydrochemical composition at different depths under reclaimed water irrigation during dry season and wet season; and (2) to identify the key factors controlling groundwater hydrochemistry seasonal variation from natural and anthropogenic perspectives. Furthermore, when seasonal influences are considered, the results can be used to evaluate the sustainability of current agricultural practices and used as guidelines for promoting water management efficiency.

STUDY AREA

The study area (Figure 1) extends over 1,918 km^2 and includes the Daxing and Tongzhou administrative districts. It is located in a southern suburb of Beijing, China and lies on the alluvial plain of the Yongding River and Chaobai River from 39°53′N to 39°55′N and from 116°23′E to 116°53′E. It is connected to the North China Plain to the south, and its western boundary coincides with the Yongding River and northeastern boundary meets the Chaobai

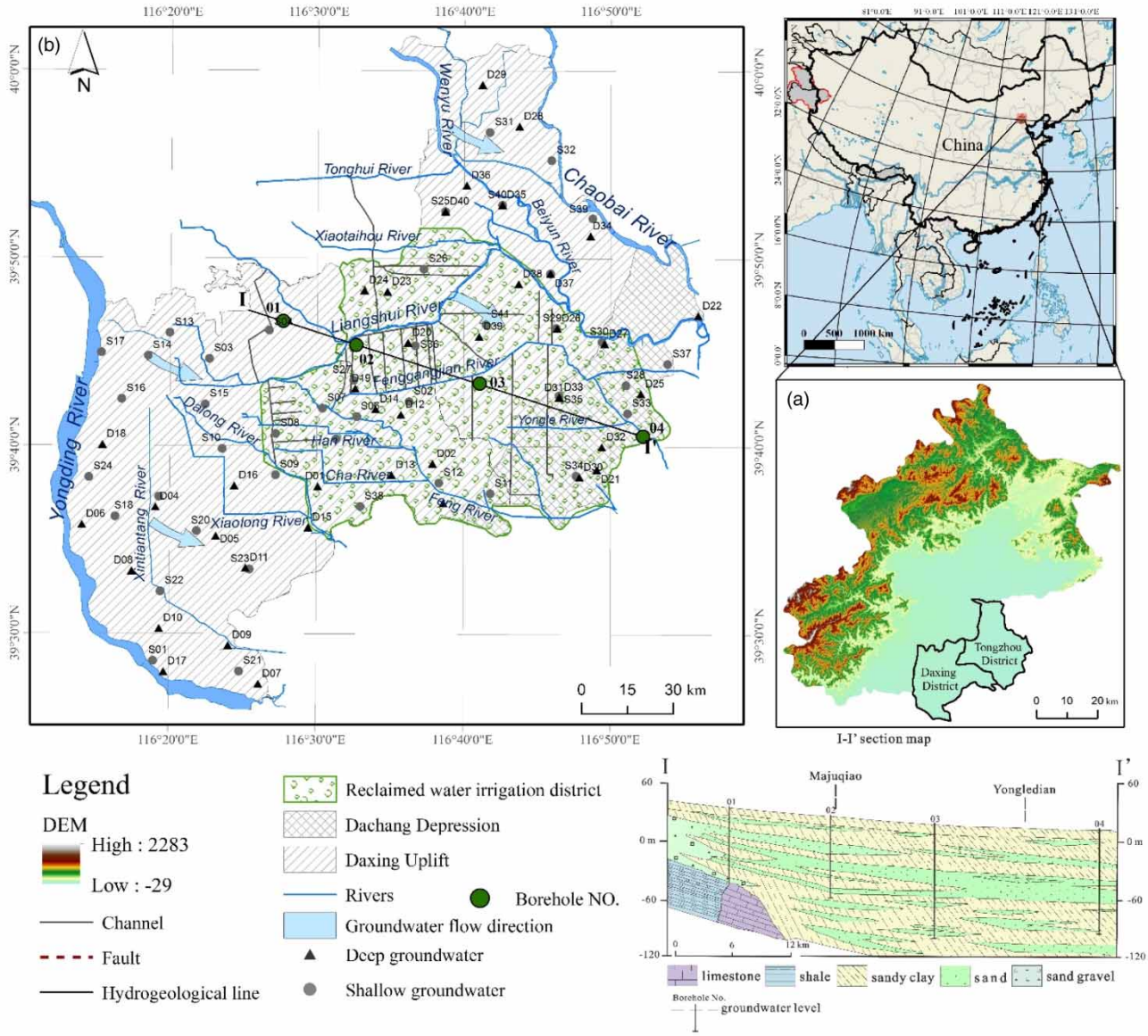

Figure 1 | Location map of study area (a) and spatial distribution of samples, as well as hydrogeological map (b), hydrogeological cross section map of I-I′ in map B at bottom right.

River. The area also encompasses a 789 km^2 of typical reclaimed water irrigation district called Southeast Reclaimed Water Irrigation Region (SRWIR), a network of rivers and irrigation ditches distributed for agricultural activities. SRWIR, as one of the largest reclaimed water irrigation regions in China, is characterized by intense greenhouse vegetable or fungus planting that accounted for more than 50% of the planting area of Beijing. Wastewater irrigation was adopted from 1969 to 2002, and second-treated wastewater (reclaimed water) has been used thereafter. So far, an annual reclaimed water amount of 0.3 billion m^3 has been applied to 2,347 km^2 irrigation area.

The study area has a typical temperate continental climate with hot and rainy summers and cold and dry winters. The yearly average temperature is 11.7 °C and long-term annual potential evaporation of up to 1,180 mm, as estimated through the Penman-Monteith equation. The mean annual precipitation of the area was 580 mm from 1951 to 2010 (Zhai *et al.* 2012) and mainly concentrated

from June to September. Furthermore, the summer maize–growing season is consistent with rainy season. Meanwhile, insufficient rainfall amounts and excessive evaporation cause severe pressure on local water resources.

The study area is divided into two geologic units, namely, Dachang Depression, which covers nearly 250 km^2 in the southeast of Tongzhou district, and Daxing Uplift, which covers the rest of the area. A fault lies in a northeast to southwest direction parallel to the boundary between the geological structures, as shown in Figure 1(b). Quaternary sediments gradually increase from northwest to southeast (maximum thickness of nearly 300 m) and exhibit incompact alternation of medium-fine sand, sandy clay, and sandy gravel aquifer (Figure 1). The multilayered aquifer results from the Yongding River and Chaobai River alluviation flowing through Xi Mountain and North Mountain, separately, show a continuous aquitard at a depth of 80 m, and separates into a shallow and deep aquifer (Chen *et al.* 2004). Distributed quaternary unconsolidated porous groundwater system are mainly recharged with precipitation, irrigation return flow, river bed infiltration and lateral flow, and are discharged with groundwater pumping, evaporation and lateral flow. According to the China Geological Survey, water yield property varies in a range of 1,000–3,000 m^3/d at the study aquifer and groundwater level alters from 4 to 28 m flowing from northwest to southeast (Wu *et al.* 2014). The hydraulic conductivity varies from 300 m/d (northwestern) to less than 10 m/d (southeastern) (Hao 2011), with an average of 12.5 m/d. Quartz, potassium feldspar, and hornblende are the dominant minerals in the deep aquifer. Calcite and dolomite are commonly present in the Quaternary strata, and illite, kaolinite, anorthose, montmorillonite and fluorite are observed (Aji *et al.* 2008). The major soil types include Brown Fluvo-aquic soil, Sajong soil, and some scattered alluvial soil. Constituting 33.81% of the grain-producing area in Beijing, the study area is mainly cultivated for winter wheat, summer maize, and greenhouse vegetables. Due to the dry climate in early spring, more than 70% of irrigation water resources were used for winter wheat (Li *et al.* 2005). Therefore, major reclaimed water was irrigated during the winter wheat-growing season.

MATERIALS AND METHODS

Sampling campaigns were performed in April (dry season) and September (wet season) in 2014. A total collection of 164 groundwater samples was collected from 42 shallow and 40 deep monitoring wells during two seasons separately. The sampling sites are shown in Figure 1(b), where S and D represent the shallow groundwater at depth <80 m and deep groundwater at depth greater than 80 m, respectively. The reclaimed water data from three WTPs in 2014 were employed as comparative standards not presented in this study. Seasonal sampling was selected to identify primary processes that control groundwater hydrochemistry variation and assess the effects from reclaimed water under SRWIR. An inductively coupled plasma atomic emission spectrometer (iCAP7400 ICP-OES) was used to detect potassium, calcium, sodium and magnesium. Anion (F, Cl, SO_4^{2-}, NO_3^-) analysis of water samples was conducted on an ion chromatography system (ICS1000). HCO_3^- and CO_3^{2-} were determined by titration with 0.02 N sulfuric acid, and methyl orange endpoint titration was used with the final pH of 4.2–4.4. For NO_2^- and NH_4^+, a DR 6000^{TM} UV-VIS Spectrophotometer was used. Total bacterial counts were determined by low temperature biochemical incubator (Prandt SPX-350FT). Groundwater chemical indicators in accord with the corresponding analysis method were measured in the laboratories of Beijing Center for Physical and Chemical Analysis.

Piper diagram was used to investigate the hydrochemical facies and major ions abundance orders. Descriptive statistics (maximum, minimum, mean, and standard deviation) and correlation coefficient analyses were performed using statistical software package (SPSS 21.0) to reveal the links between individual variables and assess the key seasonal controlling factors. The ionic ratio was useful in providing insights into the geochemical processes controlling water quality variation. For the evaluation of the equilibrium degree between water and respective minerals, saturation indices (SIs) for gypsum, halite, dolomite, and calcite were calculated on PHREEQC (2.18.00). SI is equal to 0 when groundwater is saturated, <0 when under-saturated, and >0 when over-saturated with respect to the given mineral.

RESULTS

The descriptive statistics of hydrochemical data for shallow groundwater (SGW) and deep groundwater (DGW) are separately summarized in Table 1. The basic statistical features between the two seasonal groups of groundwater were graphically visualized through box plots, which helped uncover underlying structures and detect outliers, as showed in Figure 2 and later in Figure 3. Deep groundwater ionic characteristics showed lower concentrations and tighter distributions than those of shallow groundwater. Furthermore, owing to spatial heterogeneity, groundwater chemical characteristics varied among different sampling sites. Bicarbonate and nitrate content and electrical conduction (EC) showed the highest variance in the range of their concentrations. Except for outliers, the compositions of Na^+, NO_3^-, and total bacteria count (TBC) parameters presented a slight increase, whereas no remarkable change in other ionic concentrations was observed during sampling (Figure 2).

Seasonal variation in hydrochemical characteristic of shallow groundwater

The summary of physical, chemical and microbial compositions of groundwater samples during wet season and dry seasons are provided in Table 1. Overall, the shallow groundwater showed neutral to slightly alkaline nature with pH varying from 7.0 to 8.6 with an average of 7.6. No significant variation was observed between the two seasons. The shallow groundwater EC values for dry season varied from 521 to 3,270 μS/cm with an average of 1,167 μS/cm and characterized by low values ranging from 453 to 2,001 μS/cm with an average of 1,077 μS/cm during the wet season. Similarly, highly correlated with EC, the total dissolved solids (TDS) value displayed an identical trend. The ionic composition in shallow groundwater was dominated by Na^+ (3.85–375.00 mg/L), Ca^{2+} (19.30–191.00 mg/L), Mg^{2+} (5.10–161.00 mg/L), Cl^- (11.60–348.00 mg/L), SO_4^{2-} (13.60–271.00 mg/L), and HCO_3^- (61.00–822.00 mg/L). With respect to seasonal variation, both the maximum and average ions compositions, including K^+, Ca^{2+}, Mg^{2+}, Cl^-, SO_4^{2-}, F^-, NO_2^-, and NH_4^+, in dry season were greater than those in wet season and thus are consistent with EC and TDS values. The Na^+ (71.40 mg/L), HCO_3^- (442.05 mg/L), and NO_3^- (20.31 mg/L) mean concentrations in dry season slightly increased to 80.40, 468.34 and 34.80 mg/L, respectively, in the wet season. The NO_2^- and NH_4^+ concentrations in groundwater were relatively low and below the contaminant level, except for NH_4^+ concentration in S42 and S40 wells during the dry season. About 17% of the studied shallow groundwater samples, with one deep groundwater sample (D30 with NO_3^- concentration of 72.19 mg/L in wet season) had NO_3^- levels above the health threshold of 50 mg/L for drinking water (WHO 2006). 17% and 21% of shallow groundwater samples in the dry and wet season, respectively, exceeded the maximum admissible nitrate concentration limit. Nitrate levels in wet season were higher than in dry season (Table 1). TBC, as biological indicator for fecal surface contamination, had a mean value of 44 CFU/ml in wet season and 19 CFU/ml in dry season. Generally, the shallow groundwater hydrochemical concentrations in wet season are lower than those in dry season. Dilution effect caused by fresh groundwater recharge (mainly from precipitation or irrigation water infiltration) was the predominant process, where enhanced weathering minerals during wet season are percolated down into the aquifers and the elevated levels were then retained in the subsequent dry season (Singh *et al.* 2014).

Shown in the Piper plot (Figure 4), with respect to cations, shallow groundwater samples are scattered at all zones on the lower-left trilinear plot, indicating that more than 70% samples belong to the mixed type and contain small amounts of calcium, magnesium, and sodium types. In the anion trilinear plot on the lower-right, zone E represents bicarbonate and zone B represents the mixed type. Approximately 90% and 10% of the samples were observed in zones E and B, respectively, except during dry season, where S34 with sulfate type was detected. In the central diamond-shaped field, bicarbonate was predominant in about 80% samples at zone 5, alkaline earths prevailed in dry season (zone 1), weak acids were prevalent in wet season (zone 3), and mixed-type were dominant in the other samples at zone 9. In addition, major chemical constituent variations occurred in wells S34 and S28 in which hydrochemical facies seasonally changed from HCO_3-Cl-Na-Ca to SO_4-Cl-Na-Mg and from Cl-SO_4-Ca-Mg to HCO_3-SO_4-Mg-Na, respectively. While in the shallow aquifer, HCO_3-Ca-Mg, HCO_3-Mg-Ca, HCO_3-Na-Mg-Ca, HCO_3-Ca-Mg-Na, and HCO_3-Mg-Na were the primary types along the flow direction. Overall, from April to September, the shallow groundwater

Table 1 | Statistical summary of hydrochemical parameters of reclaimed water, shallow and deep groundwater in dry and wet seasons

	pH	T (°C)	EC (μS/cm)	K^+ (mg/L)	Na^+ (mg/L)	Ca^{2+} (mg/L)	Mg^{2+} (mg/L)	Cl^- (mg/L)	SO_4^{2-} (mg/L)	CO_3^{2-} (mg/L)	HCO_3^- (mg/L)	F^- (mg/L)	NO_3^- (mg/L)	NO_2^- (mg/L)	NH_4^+ (mg/L)	TDS (mg/L)	TBC[a] CFU/ML
Reclaimed water					Total ($n = 3$)												
Max	7.9	19.7	1576	21.80	137.00	105.00	42.90	174.00	109.00		313.00	0.34	24.10				
Min	7.2	18.9	1027	18.20	79.80	65.30	27.10	96.50	89.60		164.00	0.32	22.20				
Mean	7.5	19.3	1310	19.80	107.60	84.70	35.07	143.50	98.93		227.67	0.33	23.07				
Std	0.3	0.3	224	1.50	23.38	16.22	6.45	33.72	7.94		62.73	0.01	0.79				
Shallow groundwater					Total ($n = 84$)												
Max	8.6	28.0	3270	15.20	375.00	191.00	161.00	348.00	271.00	17.50	822.00	1.70	281.66	2.62	9.51	2015	152
Min	7.0	8.0	453	0.39	3.85	19.30	5.10	11.60	13.60	0.00	61.00	0.20	0.71	0.00	0.03	275	0
Mean	7.6	16.0	1119	2.42	75.64	90.04	52.54	74.29	95.98	1.45	454.44	0.59	25.02	0.06	0.42	728	30
Std	0.4	4.4	407	2.41	50.74	39.42	28.49	53.29	99.01	4.08	162.23	0.30	45.90	0.29	1.17	274	28
Dry season ($n = 42$)																	
Max	8.6	18.0	3270	15.20	375.00	191.00	161.00	348.00	233.00	15.00	820.00	1.70	131.97	2.62	9.51	2015	74
Min	7.0	8.0	521	1.06	3.85	19.30	8.44	12.20	15.60	0.00	61.00	0.20	0.71	0.00	0.03	276	0
Mean	7.6	12.6	1167	2.55	71.40	94.61	55.85	80.93	108.86	0.57	442.05	0.61	20.31	0.09	0.55	744	19
Std	0.3	1.8	443	2.17	62.57	40.12	27.58	60.43	128.87	2.64	186.36	0.32	30.09	0.40	1.55	294	18
Wet season ($n = 42$)																	
Max	8.4	28.0	2001	13.40	167.00	159.00	126.00	187.00	271.00	17.50	822.00	1.30	281.66	0.27	2.95	1194	152
Min	7.1	11.0	453	0.39	15.60	21.50	5.10	11.60	13.60	0.00	178.00	0.20	0.71	0.00	0.03	275	2
Mean	7.7	19.4	1077	2.50	80.40	85.70	49.98	69.10	85.79	2.63	468.34	0.58	34.80	0.04	0.36	713	44
Std	0.4	3.9	381	3.04	37.13	39.63	30.96	46.85	58.07	5.32	145.20	0.30	66.71	0.07	0.67	260	36
Deep groundwater					Total ($n = 80$)												
Max	8.6	27.6	2440	5.65	358.00	94.20	104.00	300.00	654.00	24.50	544.00	2.20	72.19	0.09	1.02	1611	363
Min	7.4	10.0	435	0.37	2.31	11.70	1.96	7.50	5.11	0.00	190.00	0.20	0.71	0.00	0.03	272	0
Mean	7.9	16.7	625	1.68	59.84	44.21	17.64	28.07	55.60	4.12	288.61	0.62	3.53	0.01	0.18	390	22
Std	0.3	4.3	222	0.86	47.20	15.52	12.36	33.63	70.24	6.11	63.80	0.40	8.24	0.01	0.25	148	44
Dry season ($n = 40$)																	
Max	8.4	16.0	901	5.65	110.00	73.20	34.40	89.60	143.00	12.30	427.00	2.20	16.08	0.03	1.02	516	363
Min	7.4	10.0	483	1.04	2.31	11.70	3.83	9.40	5.11	0.00	190.00	0.30	0.71	0.00	0.03	272	0
Mean	8.0	13.2	624	2.02	43.35	43.58	17.08	27.69	51.75	2.20	286.70	0.66	3.04	0.01	0.26	369	30
Std	0.3	1.9	103	1.09	29.81	15.35	7.95	18.52	26.89	3.36	63.60	0.44	3.74	0.01	0.31	60	86
Wet season ($n = 40$)																	
Max	8.6	27.6	2440	3.08	358.00	94.20	104.00	300.00	654.00	24.50	544.00	2.10	72.19	0.09	0.79	1611	90
Min	7.6	12.0	435	0.37	19.40	13.90	1.96	7.50	6.32	0.00	198.00	0.20	0.71	0.00	0.03	276	2
Mean	7.9	20.2	631	1.39	74.84	44.82	18.30	29.52	59.67	6.35	293.35	0.61	4.33	0.01	0.13	411	30
Std	0.3	2.9	300	0.69	55.60	16.91	15.88	44.94	96.71	7.47	67.69	0.42	11.17	0.01	0.19	199	24

[a]TBC = total bacterial count, with unit of colony forming unit in 1 ml solution.

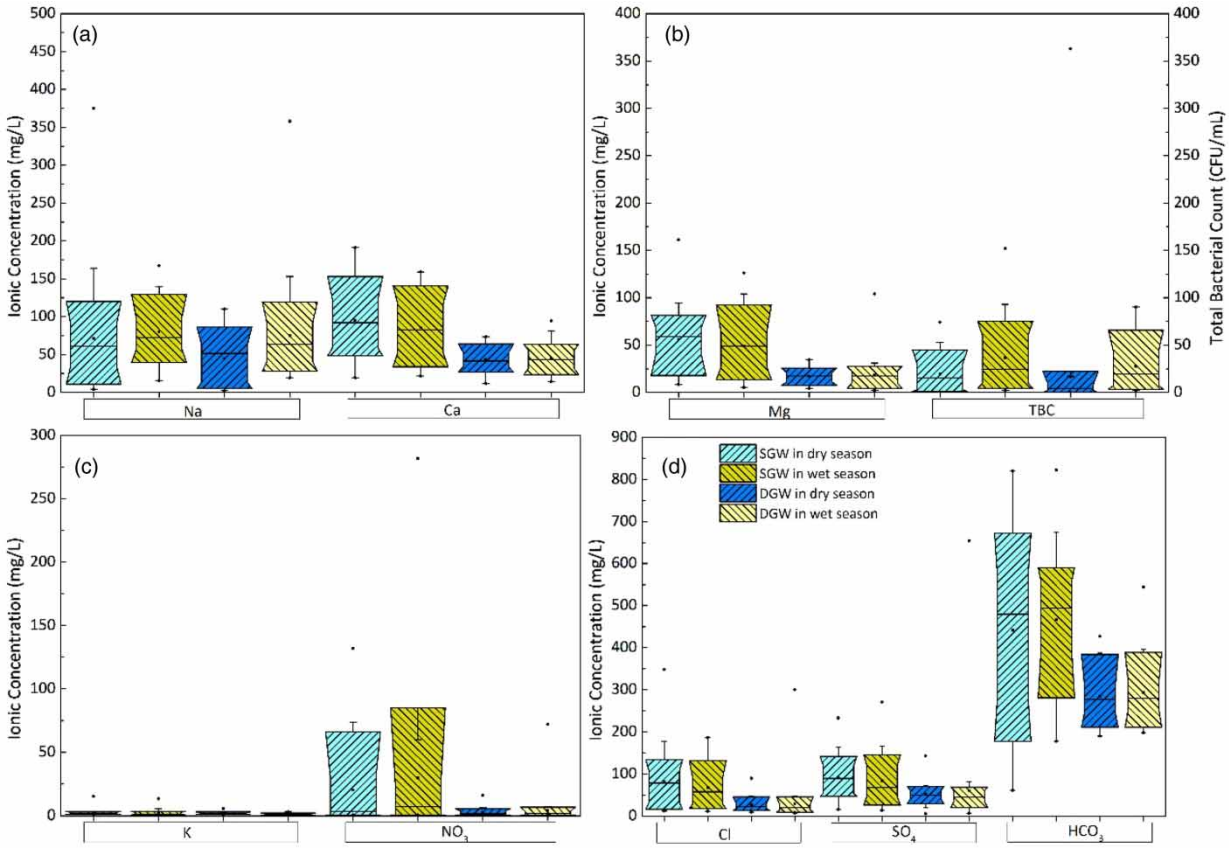

Figure 2 | Box plots of chemical major components measured in shallow aquifer and deep aquifer for dry season and wet season. Lines within the boxes, boundaries, whiskers and dots mark the median, 25th–75th percentiles, 10th–90th percentiles, and outliers, respectively.

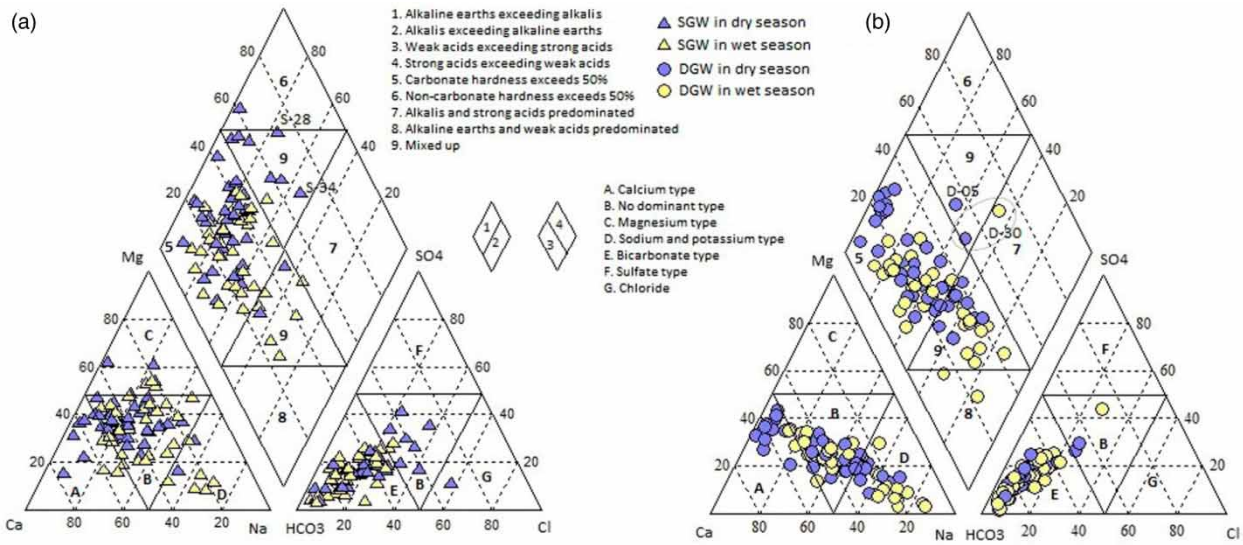

Figure 3 | Piper diagram of groundwater in (a) shallow aquifer and (b) deep aquifer.

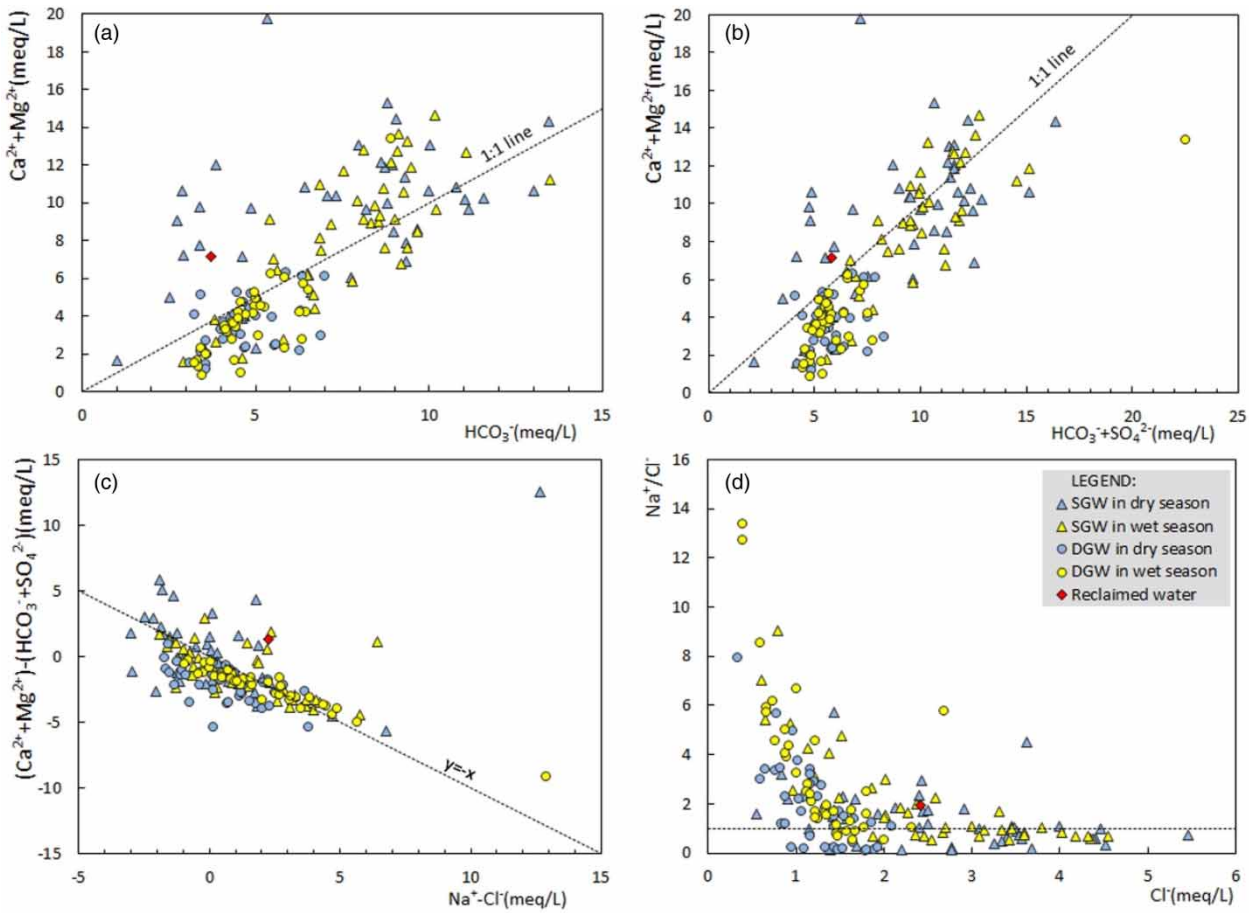

Figure 4 | Plots of ionic ratio between different cations and anions: (a) $(Ca^{2+} + Mg^{2+})$ versus HCO_3^-; (b) $(Ca^{2+} + Mg^{2+})$ versus $(HCO_3^- + SO_4^{2-})$; (c) $(Ca^{2+} + Mg^{2+})$-$(HCO_3^- + SO_4^{2-})$ versus (Na^+/Cl^-); and (d) Na^+/Cl^- versus Cl^-.

types presented generally towards sodium increase in cations and bicarbonate domination in anions. Additive sources may enter the aquifer for the elevated sodium proportions.

The correlation coefficients of all the major hydrochemical parameters for shallow groundwater in dry and wet seasons in Table 2 and Table 3, as well as in Table 4 and Table 5, were used to represent deep groundwater during different seasons. Electrical conductivity is commonly used to determine the total concentrations of ionized constituents in natural water. The major ions (Na^+, Ca^{2+}, Mg^{2+}, Cl^-, and SO_4^{2-}) were positively correlated with EC and TDS and greatly contributed to EC and TDS values. During the dry season, the 0.74 coefficient between Na^+ and Cl^- in shallow groundwater indicated halite dissolution, and the 0.81 coefficient between Na^+ and SO_4^{2-} revealed Glauber's salt ($Na_2SO_4{\cdot}10H_2O$) dissolution or cation exchange after gypsum or anhydrite weathering. Mg^{2+} and Cl^- showed good relationship at coefficient of 0.76 possibly because of Cl^- and Mg^{2+} concentration abundance or cation exchange after halite dissolution. The good correlation between Mg^{2+} and SO_4^{2-} during the wet season may indicate fertilizer leaching, which contributes such ions to groundwater. However, no clear correlation between cation and anion was observed in the wet season. In recharging groundwater with fresh water, the dilution effect greatly affected ionic composition in wet season and thus resulted in decreased correlation during bivariate analysis.

Seasonal variation in hydrochemical characteristic of deep groundwater

The mean pH value in deep groundwater (7.9) was 0.3 higher than that in shallow aquifer (7.6), which was alkaline

Table 2 | Pearson correlation coefficients of major hydrochemical parameters in shallow groundwater for dry season

2014S	EC	K^+	Na^+	Ca^{2+}	Mg^{2+}	Cl^-	SO_4^{2-}	CO_3^{2-}	HCO_3^{2-}	F^-	NO_3^-	NO_2^-	NH_4^+	TDS
EC	1.00													
K^+	0.11	1.00												
Na^+	0.77**	−0.16	1.00											
Ca^{2+}	0.61**	0.21	0.22	1.00										
Mg^{2+}	0.83**	−0.12	**0.71****	0.46**	1.00									
Cl^-	0.80**	−0.03	**0.74****	0.45**	**0.76****	1.00								
SO_4^{2-}	0.79**	0.04	**0.81****	0.32*	**0.69****	**0.85****	1.00							
CO_3^{2-}	−0.20	0.00	−0.16	−0.33*	−0.27	−0.20	−0.09	1.00						
HCO_3^{2-}	0.37*	−0.12	0.36*	0.46**	0.43**	0.15	0.00	−0.37**	1.00					
F^-	0.34*	−0.14	0.41**	−0.13	0.34*	0.38*	0.45**	0.18	−0.13	1.00				
NO_3^-	0.42**	0.02	0.25	0.26	0.34*	0.40**	0.32*	−0.14	−0.05	0.12	1.00			
NO_2^-	0.17	0.01	0.05	−0.03	0.22	0.14	0.02	−0.04	0.04	0.18	0.56**	1.00		
NH_4^+	0.03	0.53**	−0.17	0.09	−0.08	0.01	−0.03	−0.04	0.04	0.03	−0.15	−0.04	1.00	
TDS	0.93**	0.16	0.70**	0.70**	0.87**	0.85**	0.80**	−0.26	0.43**	0.32**	0.40**	0.12	−0.02	1.00

*Correlation is significant at the 0.05 level.

**Correlation is significant at the 0.01 level; correlation coefficients >0.05 are marked by bold font.

Table 3 | Pearson correlation coefficients of major hydrochemical parameters in shallow groundwater for wet season

2014S	EC	K^+	Na^+	Ca^{2+}	Mg^{2+}	Cl^-	SO_4^{2-}	CO_3^{2-}	HCO_3^{2-}	F^-	NO_3^-	NO_2^-	NH_4^+	TDS
EC	1.00													
K^+	0.19	1.00												
Na^+	0.16	−0.13	1.00											
Ca^{2+}	0.17	0.17	−0.38*	1.00										
Mg^{2+}	0.33*	0.27	−0.12	**0.85****	1.00									
Cl^-	0.41**	−0.05	0.25	−0.17	−0.09	1.00								
SO_4^{2-}	0.11	−0.19	0.38*	−0.28	−0.24	**0.83****	1.00							
CO_3^{2-}	0.06	−0.02	−0.23	−0.33*	−0.39*	−0.11	−0.10	1.00						
HCO_3^{2-}	0.50**	0.32	0.03	0.35*	0.48**	−0.03	−0.27	−0.20	1.00					
F^-	0.33*	0.12	0.41**	−0.52**	−0.32*	0.26	0.18	−0.04	−0.03	1.00				
NO_3^-	−0.15	0.14	−0.28	0.50**	0.36*	−0.18	−0.25	−0.36*	0.03	−0.18	1.00			
NO_2^-	0.12	0.12	−0.34*	−0.10	−0.19	0.51	0.43**	0.28	0.05	−0.01	−0.06	1.00		
NH_4^+	0.33	−0.09	−0.27	−0.26	−0.28	0.05**	−0.15	0.50**	0.18	0.02	−0.31	0.32	1.00	
TDS	0.87**	0.17	0.42**	0.25	0.46**	0.40**	0.19	−0.15	0.52**	0.29	−0.12	−0.07	0.10	1.00

*Correlation is significant at the 0.05 level.

**Correlation is significant at the 0.01 level; correlation coefficients >0.05 are marked by bold font.

Table 4 | Pearson correlation coefficients of major hydrochemical parameters in deep groundwater for dry season

2014D	EC	K^+	Na^+	Ca^{2+}	Mg^{2+}	Cl^-	SO_4^{2-}	CO_3^{2-}	HCO_3^{2-}	F^-	NO_3^-	NO_2^-	NH_4^+	TDS
EC	1.00													
K^+	0.26	1.00												
Na^+	0.42**	−0.00	1.00											
Ca^{2+}	0.50**	0.41**	−0.30	1.00										
Mg^{2+}	0.84**	0.10	0.32*	0.27	1.00									
Cl^-	0.84**	0.32*	0.39*	0.40**	**0.66****	1.00								
SO_4^{2-}	0.63**	0.61*	0.42**	−0.47**	0.32**	**0.70****	1.00							
CO_3^{2-}	0.47**	−0.15	0.08	−0.47**	−0.46*	−0.35*	−0.17	1.00						
HCO_3^{2-}	0.71**	0.19	0.22	0.48**	**0.73****	0.46**	0.19	−0.44**	1.00					
F^-	0.27	−0.29	**0.70****	−0.53**	0.25	0.27	0.10	0.15	0.03	1.00				
NO_3^-	0.42	0.11	0.39*	0.21	0.35*	0.37*	0.50**	−0.19	0.04	0.25	1.00			
NO_2^-	0.02	0.13	0.30	−0.22	0.03	0.04	0.08	0.19	−0.09	0.18	0.15	1.00		
NH_4^+	0.08	0.52**	0.16	0.05	−0.05	0.08	0.26	0.12	0.11	0.07	0.02	0.30	1.00	
TDS	0.87**	0.33**	0.32*	0.64**	0.83**	0.74**	0.64**	0.50**	0.73**	−0.01	0.44**	0.00	−0.00	1.00

*Correlation is significant at the 0.05 level.

**Correlation is significant at the 0.01 level; correlation coefficients >0.05 are marked by bold font.

Table 5 | Pearson correlation coefficients of major hydrochemical parameters in deep groundwater for wet season

2014D	EC	K^+	Na^+	Ca^{2+}	Mg^{2+}	Cl^-	SO_4^{2-}	CO_3^{2-}	HCO_3^{2-}	F^-	NO_3^-	NO_2^-	NH_4^+	TDS
EC	1.00													
K^+	−0.14	1.00												
Na^+	0.85**	−0.49**	1.00											
Ca^{2+}	0.51**	0.41**	0.05	1.00										
Mg^{2+}	0.89**	0.19	0.53*	**0.77****	1.00									
Cl^-	0.97**	−0.19	**0.89****	0.42**	**0.81****	1.00								
SO_4^{2-}	0.96**	−0.15	**0.87****	0.39**	**0.82****	**0.98****	1.00							
CO_3^{2-}	0.22	−0.65**	0.46**	−0.09	0.01	0.23	0.21	1.00						
HCO_3^{2-}	0.72**	−0.05	0.45**	0.70**	**0.78****	0.57**	0.53**	0.23	1.00					
F^-	0.47	−0.39*	**0.71****	−0.19	0.16	0.52**	0.47**	0.38	0.26	1.00				
NO_3^-	0.93**	0.02	**0.73****	0.58**	**0.88****	**0.94****	**0.95****	0.13	0.59**	0.34**	1.00			
NO_2^-	−0.01	−0.29	0.16	−0.24	−0.16	0.07	0.08	0.30	−0.23	0.06	0.01	1.00		
NH_4^+	−0.03	0.51**	0.17	−0.07	−0.15	−0.02	−0.09	0.57**	0.20	0.01	−0.15	0.19	1.00	
TDS	0.99**	0.10	0.82**	0.52**	0.90**	0.97**	0.96**	0.17	0.71**	0.44	0.93**	−0.02	−0.05	1.00

*Correlation is significant at the 0.05 level.

**Correlation is significant at the 0.01 level; correlation coefficients >0.05 are marked by bold font.

and had high HCO_3^- proportion at equilibrium state in deep aquifer. The EC value ranged from 435 to 2,440 μS/cm with an average of 624 μS/cm, with the slight increase displayed in wet season irrespective of maximum EC value. On the whole, the cation composition was dominated by Na^+ (2.31–358 mg/L), Mg^{2+} (1.96–104.00 mg/L), and Ca^{2+} (11.7–94.2 mg/L), with average values in the order Na^+ (59.84 mg/L) > Ca^{2+} (44.21 mg/L) > Mg^{2+} (17.64 mg/L). With regard to anions, Cl^- (7.50–300.00 mg/L), SO_4^{2-} (5.11–654.00 mg/L) and HCO_3^- (190.00–544.00 mg/L) were the major ions, exhibiting the sequence of HCO_3^- (288.61 mg/L) > SO_4^{2-} (55.60 mg/L) > Cl^- (28.07 mg/L) in mean values. As for seasonal changes, the maximum and average concentrations of Na^+, Ca^{2+}, Mg^{2+}, Cl^-, SO_4^{2-} CO_3^{2-}, and HCO_3^- in dry season were slightly higher than that in wet season. Meanwhile sodium abundance developed with an evident increase in mean value from 43.35 in the dry season to 74.84 mg/L in the wet season. Increase in the sodium concentration in irrigation water may have a negative effect on soil texture. K^+, NH_4^+ and F^- concentrations in the dry season were higher than in the wet season. In the 40 deep wells studied, NO_3^- varied from the below detection limit value of 0.71 to 16.08 mg/L in the dry season and 11.60 mg/L (without outlier of 72.19 mg/L) in the wet season. No significant seasonal distinction was observed in nitrate, nitrite and ammonium concentrations in deep groundwater. For F^-, the concentration in the samples D30, D31 and D22 exceeded the WHO (2006) limit (1.5 mg/L). These particular samples are all distributed at the edge of the alluvial plain lying along the river flow direction and typically coupled with high sodium and high bicarbonate which may be caused by prolonged water–fluoride-bearing mineral interaction attributed to slow groundwater runoff (Karthikeyan & Lakshmanan 2011). The total bacterial abundance in different seasons had the identical average counts of 30 CFU/ml but of higher standard deviation calculated in the dry season (Figure 2 and Table 1).

The deep groundwater points are distributed more intensively than shallow groundwater in the Piper diagram. Cations, calcium and sodium were the major ions distributed in zone A and zone D, while a mixed type was observed in zone B. However, cationic constituent distribution in the wet season is presented without calcium type. With regard to anions, almost 96% of the samples are concentrated at zone E of the anionic triangle, with only three samples displayed in zone B of no dominant type. It can be noted that 75% of the samples are scattered at zone 5, reflecting the chemical elements of deep groundwater mainly composed of weak acids as well as bicarbonate. Nearly 23% of the samples distributed at zone 9 are considered to be the mixture results of different water types. Samples collected in the wet season do not show significant variation in anionic constituents, while samples of D30 scattered at zone 7 show a variation from mixed up in dry season to alkaline and strong acids type in wet season particularly within increased sulfate and chloride composition. Therefore, the main water types in deep groundwater are HCO_3-Ca-Mg, HCO_3-Na-Ca-Mg, HCO_3-Ca-Na-Mg, HCO_3-SO_4-Na-Ca, and HCO_3-Na. Even though Ca^{2+} and Mg^{2+} are the dominant cations and HCO_3^- is the dominant anion, Na^+ concentration poses a fundamental impact on cation constitution. Overall, ionic concentrations in wet season were greater than those in dry season, where hysteresis effects may alter this general understanding.

For deep groundwater, Na^+ and F^- have good relationships with a coefficient of 0.70, along with correlation coefficient of 0.66 and 0.73 between cation Mg^{2+} and anions Cl^- and HCO_3^-, respectively, during dry season, which presents relatively fewer processes. During the wet season, Na^+ and Mg^{2+} have good correlation with Cl^- and SO_4^{2-}, while Ca^{2+} and Mg^{2+} were well related to HCO_3^- ($R^2 = 0.70$ and $R^2 = 0.78$). NO_3^- was well correlated with Na^+ ($R^2 = 0.73$), Mg^{2+} ($R^2 = 0.88$), Cl^- ($R^2 = 0.94$), and SO_4^{2-} ($R^2 = 0.95$), respectively. The good relation between ion constituents was also observed between Mg^{2+} with SO_4^{2-} ($R^2 = 0.82$ in deep groundwater), which may manifest the infiltration downward of $MgSO_4$ fertilizer due to the extensive agriculture activities or possible gypsum dissolution followed by cation exchange (Ben Moussa *et al.* 2011; Liu *et al.* 2015). In view of the widespread occurrence of calcite and dolomite in the study area, HCO_3^- is well correlated with Ca^{2+} and Mg^{2+} in the deep aquifer, indicating carbonate mineral weathering. The high coefficients between NO_3^- with ions may further declare the relatively stable aqueous environment in the wet season due to the hysteresis effect.

The results of Pearson correlation analysis coupled with hydrochemical characteristics demonstrated some distinctions in processes between different seasons in groundwater. During the dry season, interacted behavior among ions was highlighted in relatively stagnant hydrodynamics in the shallow aquifer. However, the correlation was weakened on account of the dilution effect along with abundant precipitation and irrigation infiltration in wet season. And some pollutants (nitrate and bacteria) residing in water or soils concurrently entered the subterranean hydrological system. As a part of the regional flow system, the correlation presented inverse-seasonal results in deep groundwater compared with shallow aquifers, which was mainly caused by delayed lateral recharge from mountain and piedmont alluvial fan areas where the low permeability of the clay-rich layer restrains precipitation and irrigation water penetration in a perpendicular direction (Wu *et al.* 2014). Here, hysteresis effects play a vital role in the seasonal hydrochemical characteristics in the deep aquifer.

DISCUSSION

Certain chemical substances in solution are carried by groundwater, which are dissolved from the rocks or soils over which the waters passed. Ionic ratios and speciation-solubility calculations combining with bivariate analysis are then employed, and the results are discussed accordingly.

Impact of natural factors on groundwater chemistry

In the $(Ca^{2+} + Mg^{2+})$ versus HCO_3^- diagram, carbonate dissolution line (1:1) suggests calcite and dolomite dissolution where 62% of shallow groundwater samples with positive correlation fall above the 1:1 line, which indicates carbonate dissolution and additional process generating either an excess of $Ca^{2+} + Mg^{2+}$ (fluoride and gypsum dissolution and input of Mg-related fertilizer) or a deficit of HCO_3^-. However, most deep groundwater samples tend to plot below the carbonate dissolution line (Figure 5(a)), where $Ca^{2+} + Mg^{2+}$ are insufficient, possibly because they were consumed during ion-exchange reactions. In shallow groundwater, the correlation coefficient of $(Ca^{2+} + Mg^{2+})$ with total cation was 0.59 in the dry season and reached 0.82 in the wet season because of the accelerated dissolution of calcium and magnesium minerals through increased fresh infiltration flux (e.g. precipitation and irrigation water). As seen in Figure 5(b), shallow groundwater data points are scattered around the 1:1 line between $(Ca^{2+} + Mg^{2+})$ and $(HCO_3^- + SO_4^{2-})$, suggesting the prevalence of carbonates and gypsum dissolution in hydrochemistry evolution. Owing to the equilibrium or oversaturated status observed from substantially positive SI values (Figure 6(a) and 6(b)), calcite and dolomite which are abundantly distributed in the aquifer system are inclined to precipitate during the continuous gypsum dissolving process (SI-gypsum <0, Figure 6(c)). Simultaneous equilibrium with calcite and dolomite coupled with the under-saturation for gypsum can be attribute to dedolomitization (Han *et al.* 2015), which is intensified in wet season (coefficient of 1.1) because of increased leaching of fresh water to the shallow aquifer. In centralized scattering of deep groundwater samples, the excess of $(HCO_3^- + SO_4^{2-})$ over $(Ca^{2+} + Mg^{2+})$ may be derived from other processes, such as ion-exchange reaction.

For the samples above the equal line of Na^+/Cl^-, halite and silicate mineral weathering and cation exchange possibly occurred, and it is possible external sources of sodium were present. In this study, the small correlation coefficient between sodium and bicarbonate contradicted heavy silicate weathering. Moreover, good correlations between Na^+ and Cl^-, between Mg^{2+} and Cl^-, and between SO_4^{2-} and Cl^- in groundwater supported halite dissolution (SI-halite <0, Figure 6(d)) and downward infiltration of soil salt. Approximately 52% and 57% of samples from the shallow aquifer and 70% and 83% of the samples from deep aquifer having an Na^+/Cl^- ratio greater than 1 during dry and wet seasons, respectively. The reason can be attributed to elevated sodium content within the albite or other sodium-montmorillonite weathering and cation exchange between Ca^{2+} or Mg^{2+} and Na^+ (Figure 5(d)).

Given that the cationic exchange reaction between Na^+ and Ca^{2+} or Mg^{2+} is a vital process in governing sodium enrichment in groundwater, the samples plotted in the $[(Ca^{2+} + Mg^{2+}) - (HCO_3^- + SO_4^{2-})]$ versus $(Na^+ - Cl^-)$ diagram should form a line with a slope of -1 (Figure 5(c)). In this instance, groundwater samples scattering along the -1 slope line indicates that cation exchange mainly accounts

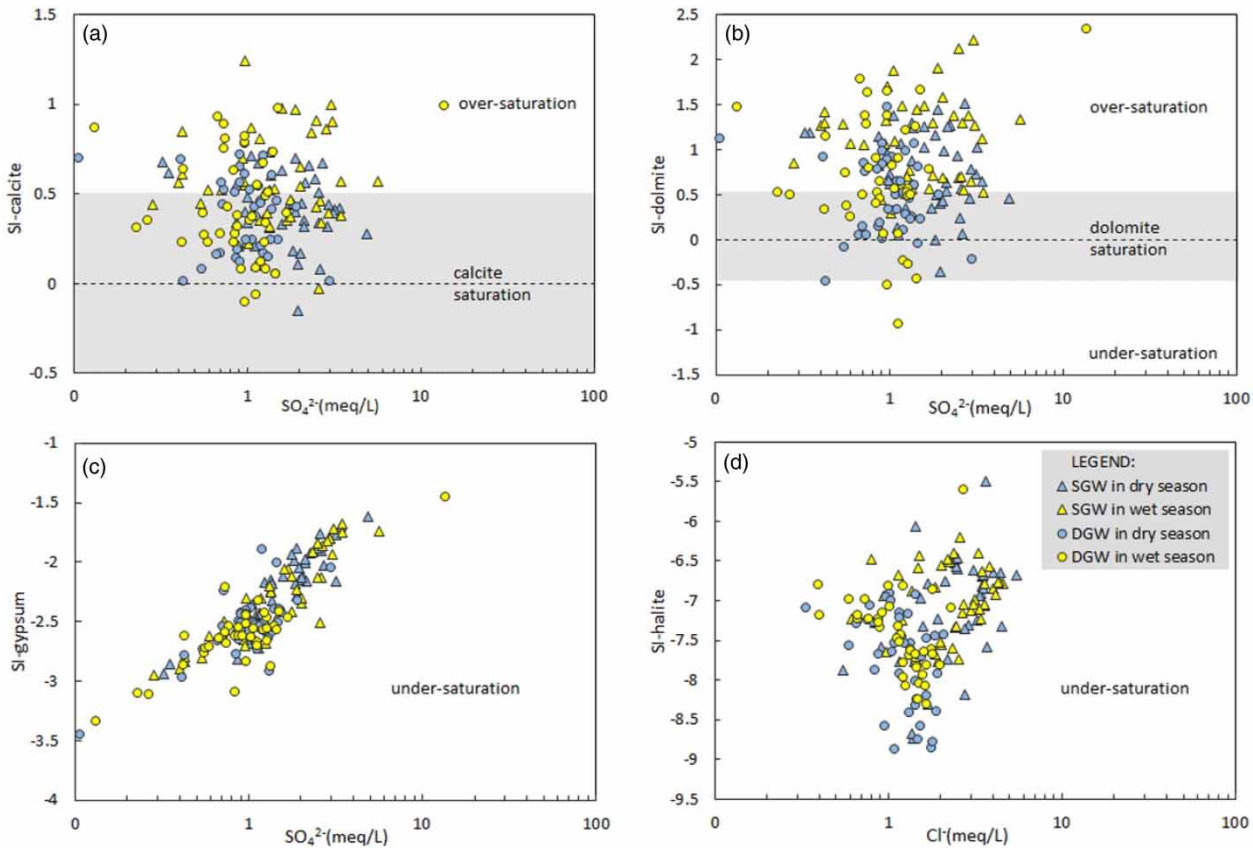

Figure 5 | Evolution of saturation indexes of (a) calcite, (b) dolomite, (c) gypsum with sulfate, and (d) saturation index of halite with chloride.

for the sodium concentration obtained in this study. In particular, a line with a slope of 0.63 ($R^2 = 0.94$) in deep groundwater was observed during the wet season, indicating the effect of cation exchange on geochemical composition at deeper aquifer. This results confirms the previous conclusion (Xing *et al.* 2013) that Ca^{2+} and Mg^{2+} in groundwater exchanges with Na^+ previously adsorbed in aquifer matrix. Meanwhile, water samples with slopes greater than −1 also illustrated other allogenic sources for excessive ($Na^+ - Cl^-$).

In summary, the saturation indexes indicated that geochemical processes, including carbonate minerals precipitation, gypsum dissolution, and halite dissolution greatly affect the chemical composition of groundwater and were analogous to the results obtained along the Yongding River alluvial fan (Huan *et al.* 2011). As indicated by the saturation interpretations and previous analysis results, mineral weathering and ion-exchange reaction associated with seasonal dilution effect greatly contribute to hydrochemistry during natural processes.

Impact of agricultural irrigation with reclaimed water on groundwater chemistry

Salinization

The evaporative extinction depth across the North China Plain is 4 m (Cao *et al.* 2013), and the direct evaporation from groundwater may not occur to elevate groundwater salinity in this region. However, successive irrigation triggers the accumulation of salt in soil formed by evaporation, which flushes soluble salts in the unsaturated zone downward to the aquifer, leading to the groundwater salinization. Furthermore, reclaimed water has a higher salinity content and organic load than other water sources and thus accelerates salinization in underground system when used for irrigation.

The salinity in reclaimed water reaches 1,310 μS/cm in EC, including 143.5 mg/L in chlorides and 2.45 in sodium adsorption ratio (SAR), as indicated by the average data of the three WTPs sampled in October 2014. The average EC

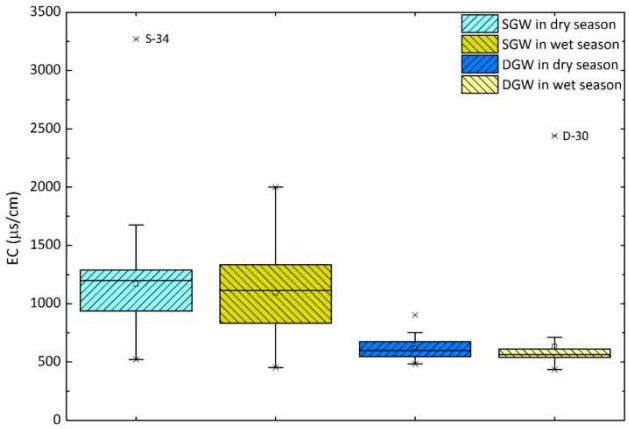

Figure 6 | Box-plots of electrical conduction (EC) in shallow and deep aquifers for dry and wet seasons.

and chloride content of tap water supplied in Beijing was 658.0 μS/cm and 21.0 mg/L, respectively (Peters *et al.* 2015). A conductivity value greater than 750 μS/cm was considered as high saline for irrigation (Wilcox 1955). Currently, most shallow groundwater samples suffer from salinity hazard at 1,119 μS/cm in EC, 74.29 mg/L in chloride, and 2.36 in SAR (Table 1). Here, the chloride concentration in shallow groundwater is lower than in reclaimed water but definitely greater than in rain water, suggesting a mixing of rain and reclaimed water leachate. Chen *et al.* (2013) conducted a field experiment demonstrating salinity accumulation in soils under years of reclaimed water irrigation. The retained salts in soil which infiltrate down toward chronic leachate from streambeds and irrigation ditches are greatly responsible for the salinization in shallow aquifer. In contrast, deep groundwater experiences less salinization with the following conditions: mean value 625 μS/cm in EC and 28.1 mg/L in chloride within minimal seasonal change. Deep groundwater had much lower EC values than shallow groundwater, but its Na^+ ions greatly contributed 41% and 54% to the major cation budget during dry and wet season, respectively, that is, deep groundwater had a higher proportion of Na^+ ions than shallow groundwater. For the Na/Cl value (Figure 5(d)), as halite dissolution surrogate, 70% of the deep groundwater samples with a value greater than 1 in the dry season, rose to 83% in the wet season. Deep groundwater is not currently subject to salinization with lower dissolved ions, but might lead to the clay particles swelling and dispersing with a high level Na^+ percentage if deep groundwater is extracted for irrigation (Frenkel *et al.* 1978; Balks *et al.* 1998; Gonçalves *et al.* 2007; Subba Rao 2008).

Nitrate contamination

Due to extensive greenhouse vegetable cultivation, excessive nitrogenous fertilizer application in Beijing is considered as the primary cause of groundwater nitrate contamination. Reclaimed water used for irrigation, rivers and ditches recharged with reclaimed water, poses additional leaching risks on groundwater nitrate contamination (Chen *et al.* 2006). Fertilizer application and reclaimed water irrigation facilitate the retention of nitrogen in soil profiles beyond the root zones. The retained nitrogen is then assimilated in the unsaturated zone where oxygen is available. Rapid flushing and leaching occur during rain events or irrigation and promote the leaching of accumulated N through the unsaturated zone to the shallow water table. Notably, elevated nitrate and chloride concentrations are observed in aquifers under the treated wastewater irrigation area. Well S34 was spatially adjacent to well D30 and both wells had Cl^- content greater than 300 mg/L, elevated SO_4^{2-} concentration, and high EC values. The positive correlation between EC and NO_3^- (Table 1) and observation wells plotted in Figure 7 indicate direct contribution of nitrate input to elevated groundwater EC.

Some shallow wells such as S03, S04, S17, S29, S32, and S36 were intensely contaminated regardless of seasonal variation (Figure 7). S03, S04, S17, S32 and S36 were located at the top zone of the alluvial fan where gravel and sand water-bearing strata are distributed. In addition, the site of S29 with high nitrate concentration located above the fault zone can be contaminated by point source pollution (Figure 1). One possible reason for continuous nitrate contaminated regions located in alluvium is the high permeability of the sediments (Andrade & Stigter 2009). Meanwhile, the prevailing source of nitrate in the aquifer was confirmed to be manure and septic waste contamination (Liu *et al.* 2014).

Even through the specific species were not detected, TBC can still be one of the major anthropogenic contamination markers from wastewater disposal or manure application. In this study, the average TBC value in shallow groundwater duplicated in wet season compared with the average TBC value in dry season, reflecting intense anthropogenic activities

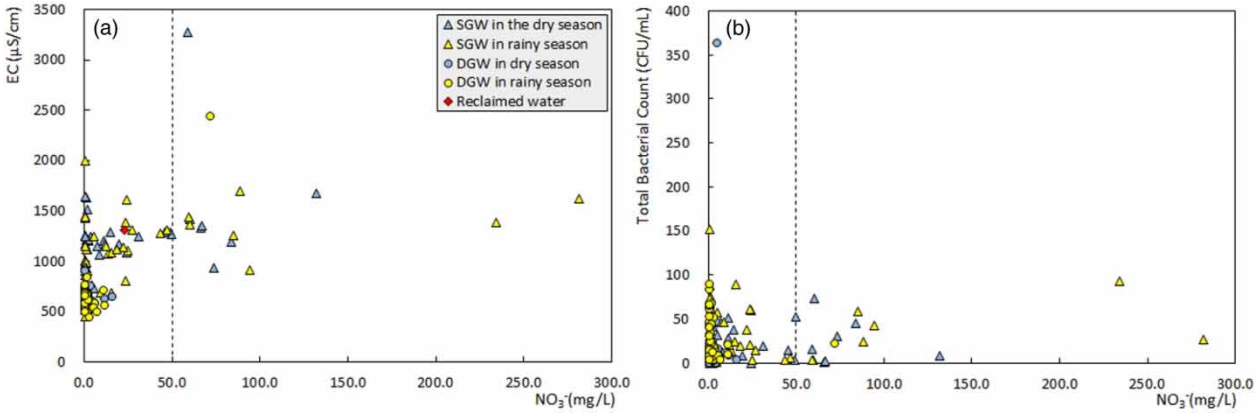

Figure 7 | Plot of evolution between (a) NO_3^- and electric conduction (EC) and (b) NO_3^- and total bacterial count (TBC).

established during the two campaigns. Meanwhile, some samples (S04 and S32) with high NO_3^- concentration and elevated TBC provide insights into reclaimed water infiltration. The results suggested that elevated nitrate contamination is caused by a mixture of local hydrogeological settings, excessive fertilizers and long-standing reclaimed water infiltration, in which some hot spots with high groundwater nitrate contents in this study area should be seriously considered.

With consideration of the seasonal variation of ion concentration in groundwater, the seasonal irrigation water resource should be different. The suggestions were proposed as follows. (1) The continuous nitrate contamination has been identified in the northern part of Daxing district. This area should establish more strict control on fertilizer and manure application in agricultural areas, and reduce the sanitary wastewater arbitrarily discharged in the municipal area. (2) With consideration of high salinity (1,119 μS/cm in EC value, 2.36 in SAR) in shallow groundwater during the dry season, shallow groundwater should not be recommended as irrigation water for winter wheat growing. (3) While in the wet season, shallow groundwater can be extracted for regular irrigation owing to the lower EC value and sodium concentration. Deep groundwater may not be suitable for long-term irrigation because of the high sodium proportion in cation ratios.

CONCLUSIONS

Based on the regional hydrogeological framework information, we conducted a hydrochemical analysis on shallow and deep groundwater samples simultaneously to assess hydrochemistry seasonal variation driven by natural and anthropogenic processes at the reclaimed water irrigation region in Beijing.

The different hydrochemical values of shallow and deep groundwater provide a transitional hydrochemical facies from Ca-Mg type to Na-Mg type. In deep groundwater, the concentration proportion of SO_4^{2-} and Cl^- anion composition increased along flow direction, but HCO_3 type still dominated. Due to the thick clay strata, the recharge condition in shallow aquifers is different from deep aquifers. Thus, the EC values and ion concentrations in groundwater at these aquifers varied with the season. The variation in chemical composition of groundwater demonstrated some complex natural processes, such as mineral weathering, cation exchange associated with dilution effect corresponding to seasonal freshwater or irrigation replenishment. Anthropogenic input into groundwater is reflected by the distribution of nitrate and salinization, which can be attributed to hydrogeological condition, overfertilization and reclaimed water irrigation in agricultural activities.

For the protection of local groundwater resources and soil from salinity hazard and nitrate contamination, water management departments should promote controlled-release fertilizer application, facilitate the improvement of treatment technologies used by WTPs, and optimize regular monitoring network for groundwater quality. Finally, the recommended suggestions should be taken into consideration bearing in mind seasonal alternation.

ACKNOWLEDGEMENTS

This research was supported by Strategic Science & Technology Project of Institute of Geographic Sciences and Natural Resources Research (Grant number: 2012ZD003). The authors would like to thank Prof. Fandong Zheng at Beijing Water Science and Technology Institute for his help. We are grateful to our colleagues for their assistance in field investigation.

REFERENCES

Aji, K., Tang, C., Song, X., Kondoh, A., Sakura, Y., Yu, J. & Kaneko, S. 2008 Characteristics of chemistry and stable isotopes in groundwater of Chaobai and Yongding River basin, North China Plain. *Hydro. Process.* **22**, 63–72.

Anane, M., Selmi, Y., Limam, A., Jedidi, N. & Jellali, S. 2014 Does irrigation with reclaimed water significantly pollute shallow aquifer with nitrate and salinity? An assay in a perurban area in North Tunisia. *Environ. Monit. Assess.* **186**, 4367–4390.

Andrade, A. I. A. S. S. & Stigter, T. Y. 2009 Multi-method assessment of nitrate and pesticide contamination in shallow alluvial groundwater as a function of hydrogeological setting and land use. *Agric. Water Manag.* **96**, 1751–1765.

Balks, M. R., Bond, W. J. & Smith, C. J. 1998 Effects of sodium accumulation on soil physical properties under an effluent-irrigated plantation. *Soil Res.* **36**, 821–830.

Ben Moussa, A., Salem, S. B. H., Zouari, K., Marc, V. & Jlassi, F. 2011 Investigation of groundwater mineralization in the Hammamet-Nabeul unconfined aquifer, north-eastern Tunisia: geochemical and isotopic approach. *Environ. Earth Sci.* **62**, 1287–1300.

Candela, L., Fabregat, S., Josa, A., Suriol, J., Vigues, N. & Mas, J. 2007 Assessment of soil and groundwater impacts by treated urban wastewater reuse. A case study: application in a golf course (Girona, Spain). *Sci. Tot. Environ.* **374**, 26–35.

Cao, G., Zheng, C., Scanlon, B. R., Liu, J. & Li, W. 2013 Use of flow modeling to assess sustainability of groundwater resources in the north China Plain. *Water Resourc. Res.* **49**, 159–175.

Cao, G., Scanlon, B. R., Han, D. & Zheng, C. 2016 Impacts of thickening unsaturated zone on groundwater recharge in the North China Plain. *J. Hydrol.* **537**, 260–270.

Carroll, S., Liu, A., Dawes, L., Hargreaves, M. & Goonetilleke, A. 2013 Role of land use and seasonal factors in water quality degradations. *Water Resour. Manag.* **27**, 3433–3440.

Chen, J., Tang, C., Sakura, Y., Kondoh, A., Yu, J., Shimada, J. & Tanaka, T. 2004 Spatial geochemical and isotopic characteristics associated with groundwater flow in the North China Plain. *Hydrol. Process.* **18**, 3133–3146.

Chen, J., Tang, C. & Yu, J. 2006 Use of O-18, H-2 and N-15 to identify nitrate contamination of groundwater in a wastewater irrigated field near the city of Shijiazhuang, China. *J. Hydrol.* **326**, 367–378.

Chen, W., Lu, S., Pan, N. & Jiao, W. 2013 Impacts of long-term reclaimed water irrigation on soil salinity accumulation in urban green land in Beijing. *Water Resourc. Res.* **49**, 7401–7410.

Foppen, J. W. A. 2002 Impact of high-strength wastewater infiltration on groundwater quality and drinking water supply: the case of Sana'a, Yemen. *J. Hydrol.* **263**, 198–216.

Frenkel, H., Goertzen, J. O. & Rhoades, J. D. 1978 Effects of clay type and content, exchangeable sodium percentage, and electrolyte concentration on clay dispersion and soil hydraulic conductivity 1. *Soil Science Society of America Journal* **42**, 32–39.

Gonçalves, R. A. B., Folegatti, M. V., Gloaguen, T. V., Libardi, P. L., Montes, C. R., Lucas, Y. C., Dias, T. S. & Melfi, A. J. 2007 Hydraulic conductivity of a soil irrigated with treated sewage effluent. *Geoderma* **139**, 241–248.

Han, D., Post, V. E. A. & Song, X. 2015 Groundwater salinization processes and reversibility of seawater intrusion in coastal carbonate aquifers. *J. Hydrol.* **531**, 1067–1080.

Hao, L. 2011 *The Groundwater Vulnerability Evaluation Method Based on RSVA Model and the Application of Beijing Plain*. Masters Thesis, China University of Geoscience, Beijing.

Huan, H., Wang, J., Jieqiong, Z. & Yuanzheng, Z. 2011 Water-rock interaction simulation of groundwater in the Yongding River alluvial fan of Beijing plain. In: *2011 IEEE International Symposium on Water Resource and Environmental Protection*, 20–22 May, Xi'an, China.

Isa, N. M., Aris, A. Z., Wan Sulaiman, W. N. A., Lim, A. P. & Looi, L. J. 2014 Comparison of monsoon variations over groundwater hydrochemistry changes in small Tropical Island and its repercussion on quality. *Hydrol. Earth Syst. Sci. Discuss.* **2014**, 6405–6440.

Jurado, A., Vàzquez-Suñé, E., Carrera, J., López de Alda, M., Pujades, E. & Barceló, D. 2012 Emerging organic contaminants in groundwater in Spain: a review of sources, recent occurrence and fate in a European context. *Sci. Tot. Environ.* **440**, 82–94.

Karthikeyan, B. & Lakshmanan, E. 2011 *Fluoride in Groundwater: Causes, Implications and Mitigation Measures.* Nova Science Publishers, Hauppauge, New York, USA.

Kass, A., Gavrieli, I., Yechieli, Y., Vengosh, A. & Starinsky, A. 2005 The impact of freshwater and wastewater irrigation on the chemistry of shallow groundwater: a case study from the Israeli Coastal Aquifer. *J. Hydrol.* **300**, 314–331.

Katz, B. G., Griffin, D. W. & Davis, J. H. 2009 Groundwater quality impacts from the land application of treated municipal wastewater in a large karstic spring basin: chemical and microbiological indicators. *Sci. Tot. Environ.* **407**, 2872–2886.

Li, J., Inanaga, S., Li, Z. & Eneji, A. E. 2005 Optimizing irrigation scheduling for winter wheat in the North China Plain. *Agricultural Water Management* **76**, 8–23.

Liu, M., Alfa-Sika, M. S., Tchakala, I., Djaneye-Boundjou, G. & Chen, H. 2014 Tracking sources of groundwater nitrate contamination using nitrogen and oxygen stable isotopes at Beijing area, China. *Environ. Earth Sci.* **72**, 707–715.

Liu, F., Song, X., Yang, L., Han, D., Zhang, Y., Ma, Y. & Bu, H. 2015 The role of anthropogenic and natural factors in shaping the geochemical evolution of groundwater in the Subei Lake basin, Ordos energy base, Northwestern China. *Sci. Tot. Environ.* **538**, 327–340.

Peters, M., Guo, Q., Strauss, H. & Zhu, G. 2015 Geochemical and multiple stable isotope (N, O, S) investigation on tap and bottled water from Beijing, China. *Journal of Geochemical Exploration* **157**, 36–51.

Re, V., Sacchi, E., Mas-Pla, J., Menció, A. & El Amrani, N. 2014 Identifying the effects of human pressure on groundwater quality to support water management strategies in coastal regions: a multi-tracer and statistical approach (Bou-Areg region, Morocco). *Sci. Tot. Environ.* **500–501**, 211–223.

Singh, K. P., Gupta, S. & Mohan, D. 2014 Evaluating influences of seasonal variations and anthropogenic activities on alluvial groundwater hydrochemistry using ensemble learning approaches. *J. Hydrol.* **511**, 254–266.

Subba Rao, N. 2008 Factors controlling the salinity in groundwater in parts of Guntur district, Andhra Pradesh, India. *Environ. Monit. Assess.* **138**, 327–341.

Surinaidu, L. 2016 Role of hydrogeochemical process in increasing groundwater salinity in the central Godavari delta. *Hydrol. Res.* **47**, 373–389.

Vorosmarty, C. J., McIntyre, P. B., Gessner, M. O., Dudgeon, D., Prusevich, A., Green, P., Glidden, S., Bunn, S. E., Sullivan, C. A., Liermann, C. R. & Davies, P. M. 2010 Global threats to human water security and river biodiversity (vol 467, pg 555, 2010). *Nature* **468**, 334–334.

WHO 2006 *Guidelines for Drinking-Water Quality: Incorporating First Addendum*. WHO, Geneva, Switzerland, 1: 515 pp.

Wilcox, L. V. 1955 *Classification and use of Irrigation Waters*. UDSA, Washington, DC.

Wu, W., Yin, S., Liu, H. & Chen, H. 2014 Groundwater vulnerability assessment and feasibility mapping under reclaimed water irrigation by a modified DRASTIC model. *Water Resour. Manag.* **28**, 1219–1234.

Xing, L., Guo, H. & Zhan, Y. 2013 Groundwater hydrochemical characteristics and processes along flow paths in the North China Plain. *J. Asian Earth Sci.* **70–71**, 250–264.

Xu, J., Wu, L., Chang, A. C. & Zhang, Y. 2010 Impact of long-term reclaimed wastewater irrigation on agricultural soils: a preliminary assessment. *Journal of Hazardous Materials* **183**, 780–786.

Yan, S.-F., Yu, S.-E., Wu, Y.-B., Pan, D.-F., She, D.-L. & Ji, J. 2015 Seasonal variations in groundwater level and salinity in coastal plain of eastern China influenced by climate. *J. Chem.* **2015**, 8.

Zhai, Y., Wang, J., Teng, Y. & Zuo, R. 2012 Water demand forecasting of Beijing using the time series forecasting method. *J. Geogr. Sci.* **22**, 919–932.

First received 23 July 2017; accepted in revised form 5 January 2018. Available online 27 February 2018